Parametric Studies for the Optimum Synthesis of Oscillating-Slide Actuators for Vertical Manipulation Applications

P.A. Simionescu, *Member, IAENG*

***Abstract*—The oscillating-slide linkage, symbolized RPRR is one of the most utilized inversions of the slider-crank mechanism. This paper considers the cases where the rocker of an RPRR mechanism is loaded primarily by gravitational forces, like in boom cranes, dump trucks and aerial-work platforms. In all these applications, in addition to satisfying imposed limit positions, minimizing the peak actuator force over the working range of the mechanism is the main requirement. An optimization problem is defined and the dual solutions to this problem i.e. a short-rocker and a long-rocker RPRR mechanism, are summarized in the form of parametric charts, performance charts and design recommendations. Also observed via bivariate plots are the ensuing transmission angle, mechanical advantage and input-output linearity error of these optimum mechanism solutions. Together, these plots (each consisting of thousands of points obtained through repeated optimization) allow for a rapid overview upon the capabilities of the RPRR mechanism, being additionally useful in guiding the designer's decision when flexibility exists in choosing the extension coefficient of the actuator, or the angle of swing of the rocker is not imposed a strict value.**

***Index Terms* — payload manipulation, slider-crank inversion, limit positions, kinetostatics, objective function, optimization.**

I. Introduction

ONE of the most used inversions of the planar slider-crank linkage is the oscillating-slide mechanism with translating input, symbolized RPRR, where the underscore indicates a powered prismatic joint. It serves to convert the input motion of a linear actuator into swing motion of the output-link, called rocker [1-4]. In many applications such as boom cranes, patient-transfer lifts, engine hoists, telescopic handlers, forklift trucks, skip loaders, dump trucks, aerial-work platforms, see Fig. 1 and references [5-9], the output-link is loaded by downward gravitational forces only, either of the rocker itself, or in combination with a payload.

The main requirement upon most RPRR applications is to attain prescribed limit angles of the rocker, as the actuator extends from its minimum length (L_{min}) to its maximum length (L_{max}). The synthesis of the centric RPRR mechanism for imposed rocker angles φ_s and φ_f (see Fig. 2), given L_{min} and L_{max} of the linear motor, can be performed graphically [10—12]. Attaining the imposed limit positions is seldomly enough however, and a trial and error search must be conducted, until satisfactory actuator load-force and motion transmitting characteristics are achieved. Typical performance criteria observed by designers are *minimizing the actuator force*, maximizing the *mechanical advantage*, and maintain a favorable *transmission angle* [13-18]. According to [3], [4] and [19], the transmission angle in a linkage mechanism should not depart more than ±60° from the ideal value of 90°, or otherwise joints will jam. For applications where a return force or moment exists, transmission angles ranging between 15° and 165° are assumed satisfactory.

This paper discusses the synthesis of the RPRR oscillating-slide mechanism for prescribed limit positions, given the shortest and longest lengths of the linear motor,

Fig. 1. Applications of RPRR mechanism having the rocker loaded by gravitational forces only: (a) boom cranes, (b) patient-transfer lifts and engine hoists, (c) telescopic handlers (d) aerial-work platforms, (e) skip loaders, and (f) dump trucks.

Manuscript received January 5, 2020; revised April 14, 2020. This work was supported in part by the Texas Research and Development Foundation under Grant TRDF18-0217.

P.A. Simionescu is with Texas A&M University Corpus Christi, Corpus Christi, TX 78418 USA (phone: 361-825-5899; fax: 361-825-3056; e-mail: pa.simionescu@tamucc.edu).

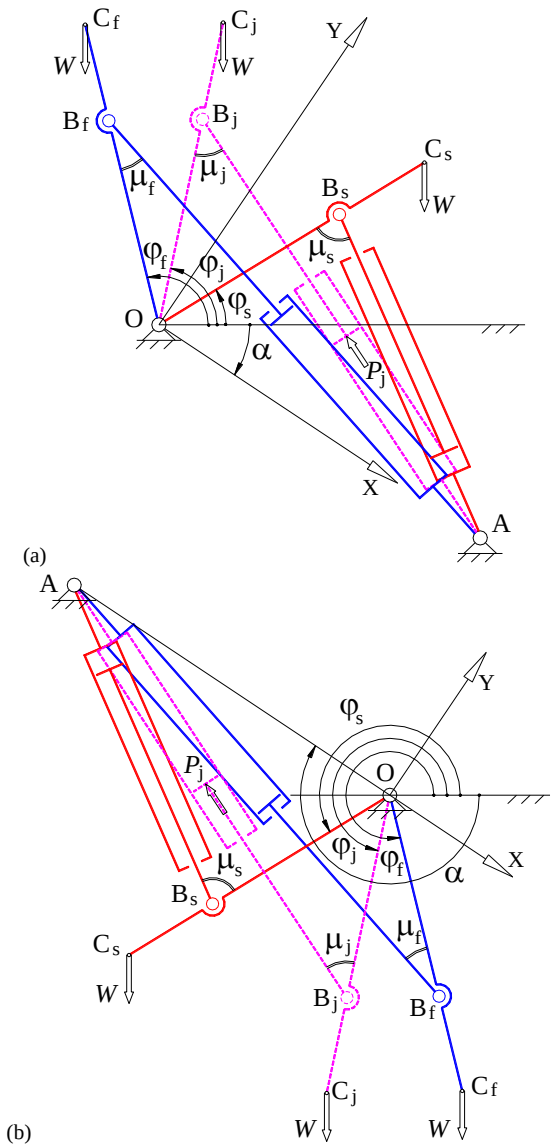

Fig. 2: RPRR oscillating-slide mechanism loaded with a constant downforce *W*, shown in its initial position 's', in its final position 'f', and in an arbitrary intermediate position 'j'. Note that in both figures, the OX axis passes through the center of ground joint A.

while simultaneously ensuring minimum actuator force when the rocker is loaded by a constant downwards force (see Fig. 2). Additionally, the following three performance parameters have been observed via bivariate plots [20]: (*i*) the deviation from 90° of the transmission angle, (*ii*) the mechanical advantage or actuator-force to load-force multiplication factor, and (*iii*) the input-output (I/O) linearity error.

The related problem of kinetostatic synthesis, coupled with position requirements, of planar four bar and slider crank mechanisms and of open kinematic chains, with application to exercise machine and assistive devices have been considered by several researchers in the past [13], [14], [23], [24], [25]. The problem of minimizing the actuator force of an actual RPRR mechanism has been studied by Shoup [21] and Beiner [22]. The latter author formulated and solved a mini-max problem analytically, which however yields suboptimal solutions for the cases where the rocker of the RPRR mechanism starts moving from a horizontal position. Neither author recognized the existence of a dual, short rocker and long rocker solution associated to a given

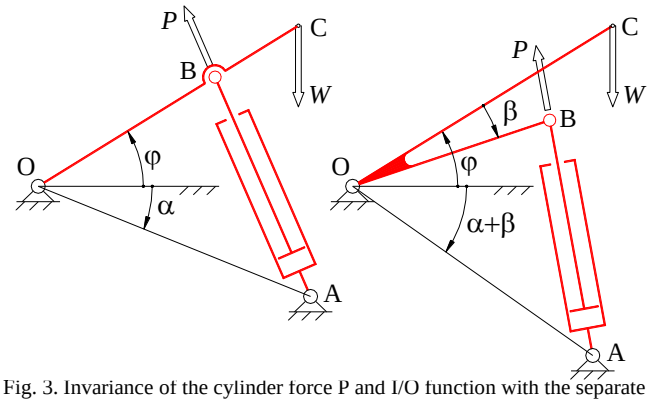

Fig. 3. Invariance of the cylinder force P and I/O function with the separate rotation by an angle β of the triangular loop O-A-B.

minimum and maximum actuator lengths L_{min} and L_{max}, as explained later in this paper with reference to equation (6).

II. Synthesis Problem Formulation

Fig. 2 depicts two RPRR oscillating-slide mechanisms loaded by a constant downward force *W*, with one mechanism being the 180° rotated image of the other one. The applied load force *W* must be overcome by a position-dependent force P_j delivered by the linear actuator. Note that, from the standpoint of actuator force history P_j (less the sign of this force), these two mechanisms are equivalent. Also note the existence of equivalent mechanism solutions which are mirror images about OY of those graphed in Fig. 2, a property also exhibited by the PRRR slider-rocker mechanisms considered in [26].

The first design requirement upon the mechanisms in Fig. 2 is to attain prescribed initial φ_s and final φ_f angles of the rocker (corresponding to an angular stroke $\Delta\varphi=\varphi_f-\varphi_s$) when the actuator extends over its full range $\Delta S_{max}=L_{max}-L_{min}$, where $L_{min}=AB_s$ and $L_{max}=AB_f$.

For added generality, the RPRR mechanisms in this paper will be assumed normalized with respect to the ground link i.e. at all times $OA = 1$. The dimensions of the actual RPRR mechanism will be obtained post synthesis through scaling. Although in most applications points O, B and C are not collinear, any such practical case is equivalent to a simplified mechanism such as those shown in Fig. 2, obtainable by applying rotation invariances as shown in Fig. 3 [6].

The first design requirement upon the mechanisms in Fig. 2 is to attain prescribed initial φ_s and final φ_f angles of the rocker (corresponding to an angular stroke $\Delta\varphi=\varphi_f-\varphi_s$) when the actuator extends over its full range $\Delta S_{max}=L_{max}-L_{min}$, where $L_{min}=AB_s$ and $L_{max}=AB_f$. The motion capabilities of the linear actuator of the mechanisms in Fig. 2 will be specified by its normalized minimum length AB_s, and by its extension coefficient *K* defined as:

$$K = L_{max}/L_{min} = 1 + \Delta S_{max}/L_{min} \quad (1)$$

Coefficient *K* can range between 1.25 and 1.8 for simple hydraulic or pneumatic cylinders, between 2.5 and 3 for piggyback cylinders, and between 3 and 4.7 for telescopic cylinders [27], [28], [29]. Telescopic cylinders with more than five stages, or of the trunnion-mount type can extend over six times their fully retracted length. The *K* values assumed throughout this paper however will not exceed 5.

In the optimum synthesis problem considered here, given are the rocker angles φ_s and φ_f, extension coefficient *K*, and

the normalized minimum and maximum lengths of the actuator AB_s and AB_f respectively. The required rocker length OB (also normalized) can be determined using the following scalar equations written about the OXY reference frame in Fig. 2:

$$(x_{Bs} - x_A)^2 + (y_{Bs} - y_A)^2 = AB_s^2 \quad (2a)$$

$$(x_{Bf} - x_A)^2 + (y_{Bf} - y_A)^2 = AB_f^2 \quad (2b)$$

where

$$x_{Bs} = OB\,cos(\varphi_s + \alpha)$$

$$y_{Bs} = OB\,sin(\varphi_s + \alpha)$$

$$x_{Bf} = OB\,cos(\varphi_f + \alpha)$$

$$y_{Bf} = OB\,sin(\varphi_f + \alpha)$$

For $x_A = 1$, $y_A = 0$ and $AB_f = K \cdot AB_s$ equations (2) become:

$$OB^2 - 2OB\,cos(\varphi_s + \alpha) + 1 = AB_s^2 \quad (3a)$$

$$OB^2 - 2OB\,cos(\varphi_f + \alpha) + 1 = (K \cdot AB_s)^2 \quad (3b)$$

After eliminating AB_s between these two equations, a quadratic equation in the unknown length OB is obtained:

$$OB^2 - 2 \cdot \vartheta \cdot OB + 1 = 0 \quad (4)$$

with solutions

$$OB = \vartheta \pm \sqrt{\vartheta^2 - 1} \quad (5)$$

where

$$\vartheta = \Big(K^2\,cos(\varphi_s + \alpha) - cos(\varphi_f + \alpha)\Big)/(K^2 - 1)$$

The "±" sign in equation (5) indicates that for a given actuator of extension coefficient K, two RPRR mechanism solutions exist [30] and [31]. The solution corresponding to "–" in front of the square root is called *short-rocker mechanism* (SR in short) while the one with "+" is called *long-rocker mechanism* (LR in short). Once the normalized rocker length OB has been determined, the corresponding normalized, fully retracted length AB_s of the actuator can be calculated with equation (3a).

Often time in practice ground joint A does not have a strictly imposed location, and consequently angle α in Fig. 2 can be adjusted until additional requirements upon the RPRR mechanism are satisfied. A *mini-max* optimization problem in the angle α can therefore be formulated:

$$P_{max} = min_{\alpha=0..360°}\big|max_{j=1..n}\big|P_j(\alpha)\big|\big| \quad (6)$$

The total number of discrete positions n correspond to actuator length AB_j taking evenly spaced values between AB_s and AB_f. For a steady load W, the required actuator force P_j in equation (6) corresponding to a current position j is calculated from the moment equilibrium of the rocker about point O:

$$P_j \cdot OB \cdot sin(\mu_j) = W \cdot OC \cdot cos(\varphi_j) \quad (7)$$

Without a loss of generality, the product $W \cdot OC$ in equation (7) can be assumed to be equal to one, case in which:

$$P_j = cos(\varphi_j)/\big(OB \cdot sin(\mu_j)\big) \quad (8)$$

where the transmission angle at position j is:

$$\mu_j = arcos\,\big(OB^2 + AB_j^2 - 1\big)/2 \cdot OB \cdot AB_j \quad (9)$$

When minimizing objective function (6), it is important to reject the cases where vector loop O-A-B changes orientation between the initial and final positions, known as *branch defective* [19]. This can be done by evaluating the vector products $\mathbf{OB}_j \times \mathbf{AB}_j$ for j=1..n, and penalizing the solutions where they have different signs [32].

In case of knuckle-boom cranes, the design criterion in equation (7) ensures the minimization of the boom actuator force, although this force will depend on the position angle of the jib (i.e. the second link of the boom crane). Relevant in this case is to best combine the displacements of the two actuators of the crane for a given payload lift path, a problem discussed in reference [33].

TABLE 1: ANGULAR STROKES FOR VARIOUS RPRR APPLICATIONS

Application	φ_s [DEG]	$\Delta\varphi$ [deg]
Hoists	-30 to -15	60 to 65
Boom cranes	-10 to 0	65 to 80
Knuckle boom cranes – boom	-10 to 0	65 to 90
Knuckle boom cranes – jib	-165 to -150	110 to 135
Telescopic handlers	-10 to 0	70 to 80
Aerial work platforms	-20 to 0	80 to 100
Fork lifts (loaded)	80 to 120	30 to 40
Skip loaders	40 to 50	90 to 110
Dump trucks	-5 to 0	60 to 75

Simultaneously with minimizing the peak actuator force in equation (6), three other parameters of concern to the designer will be monitored as follows: (*i*) deviation from 90° of the *transmission angle*

$$\delta_{max} = max_{j=1..n}\big|90° - \mu_j\big|$$

(*ii*) *mechanical advantage* (*MA*) or *actuator-force to load-force multiplication factor* [13], [14]:

$$MA = \frac{W}{P} = \left[\frac{dy_C}{d(AB)}\right]^{-1} = \frac{OB \cdot \sin(\mu)}{OC \cdot \cos(\varphi)}$$

and (*iii*) *maximum I/O displacement linearity-error*.

$$\varepsilon_{max} = \max_{j=1..n}\big|\varepsilon_j\big| = \max_{j=1..n}\left|\frac{AB_j - AB_s}{AB_f - AB_s} - \frac{\varphi_j - \varphi_s}{\Delta\varphi}\right|$$

This latter parameter because there are applications where a near-linear input-output relation $\varphi(AB_j)$ is desired to facilitate position control. In equation (12) the angle of the rocker is

$$\phi_j = cos^{-1}\big(0.5\,\big(OB^2 - AB_j^2 + 1\big)/OB\big) - \alpha$$

In applications like those in Fig. 1, the initial angle φ_s of the rocker and its maximum travel $\Delta\varphi$ are design requirements. Typical values of these two angles, extracted from references [7]. [8], [9] and other company catalogues, are listed in Table 1.

III. SYNTHESIS PROBLEM FORMULATION

The objective function in equation (6) has been minimized with respect to α using a combination of the *Localmin* univariate minimization algorithm due to Brent, preceded by a grid search [34], [35]. The number of displacement steps of the linear actuator has been considered equal to five times the angle $\Delta\varphi$ in degrees (e.g. for $\Delta\varphi$=60°, n=300).

To provide an overview upon the design space of this optimization problem, a number of bivariate parametric studies have been performed. The first set of studies done consisted of minimizing the function (7) for the more common case where in its initial position the rocker is horizontal (i.e. φ_s=0), and for $1.25 \le K \le 5$, and $30° \le \Delta\varphi \le 120°$. The resulting data served to generate the performance plots in Figs. 4 to 7, and the parametric charts in Figs. A1, A2 and A3 in Appendix 2. Note that in some of these, as well as in other subsequent 3D plots, the vertical axis, or the $\Delta\varphi$ and K axes have been reversed to provide best vintage points for the respective graphs.

The plots in Figs. 4 indicate that for small extension coefficients K, the peak actuator force P_{max} increases with the increase of $\Delta\varphi$, more so in case of SR configurations.

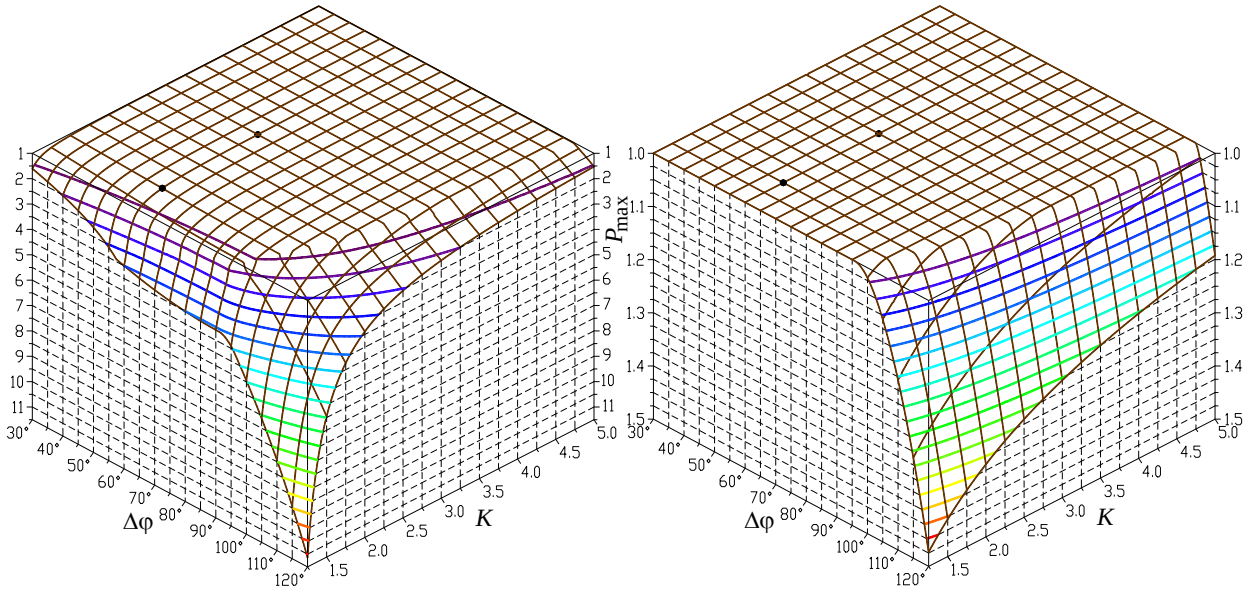

(SR) (LR)

Fig. 4: Peak actuator force of the optimum RPRR mechanisms with φ_s=0. Plot (**a**) corresponds to short rocker mechanisms and plot (**b**) corresponds to long rocker mechanisms.

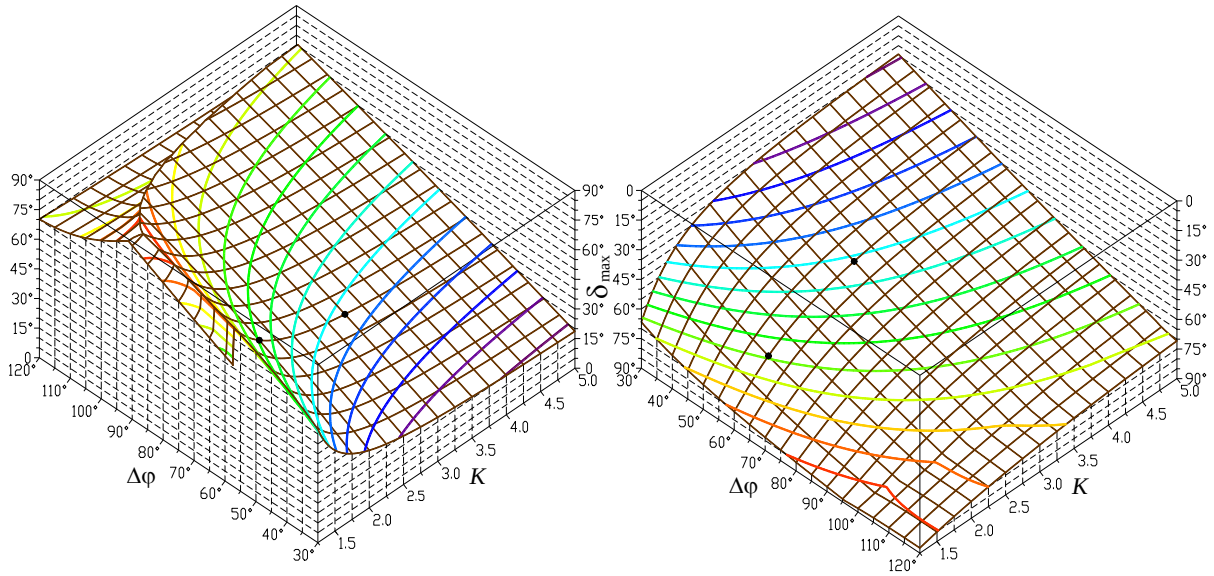

(SR) (LR)

Fig. 5: Maximum deviation from 90° of the transmission angle of the optimum RPRR mechanisms with φ_s=0.

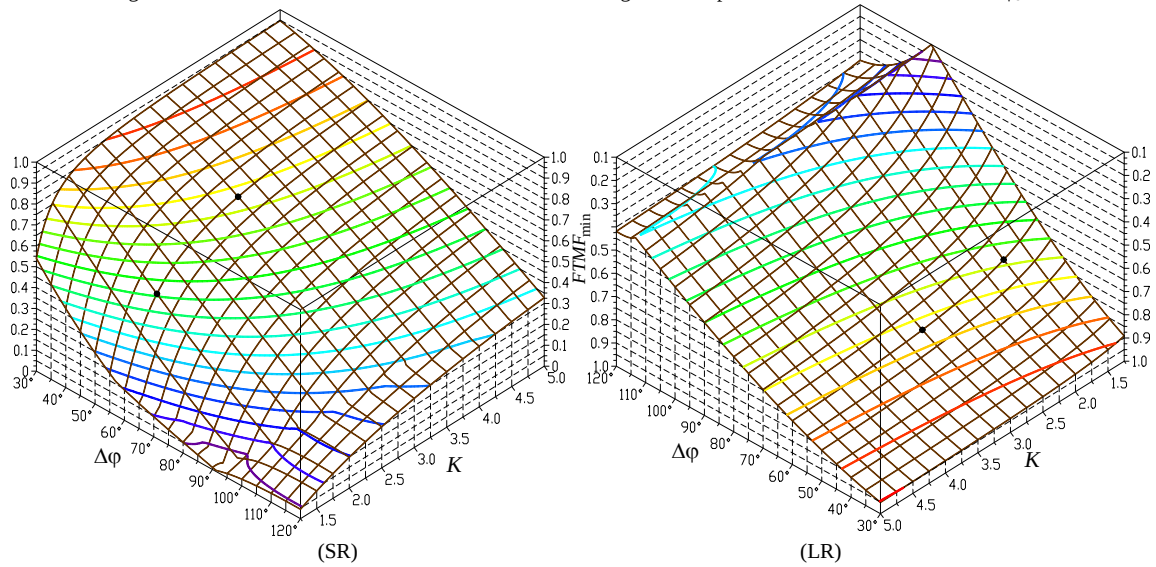

(SR) (LR)

Fig. 6: Maximum mechanical advantage of the optimum RPRR mechanisms with φ_s=0.

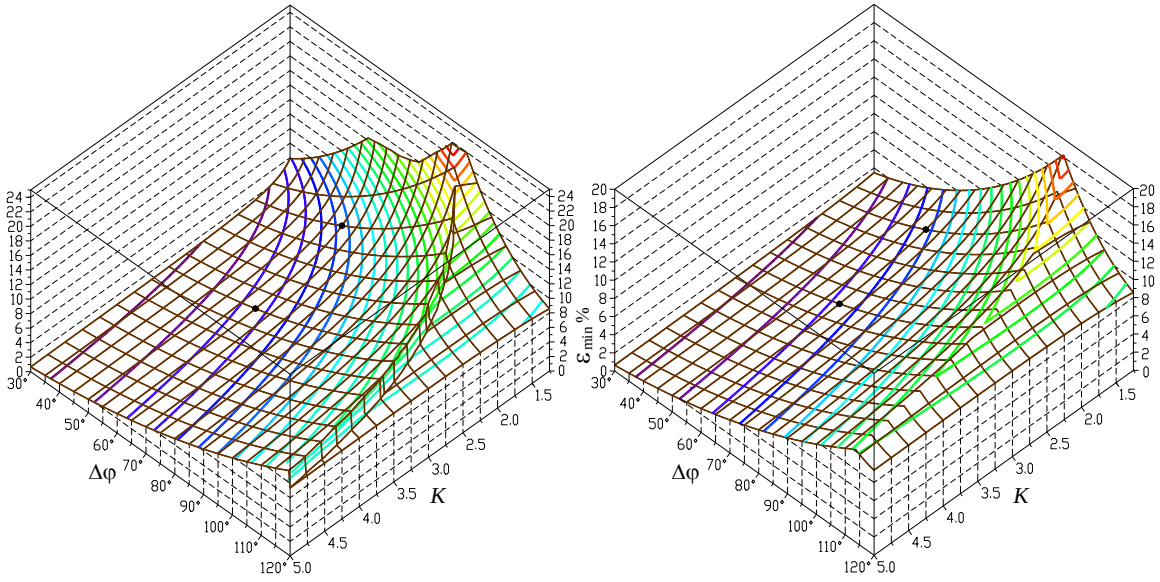

(SR) (LR)

Fig. 7: Peak actuator force of the optimum RPRR mechanisms with φ_s=0.

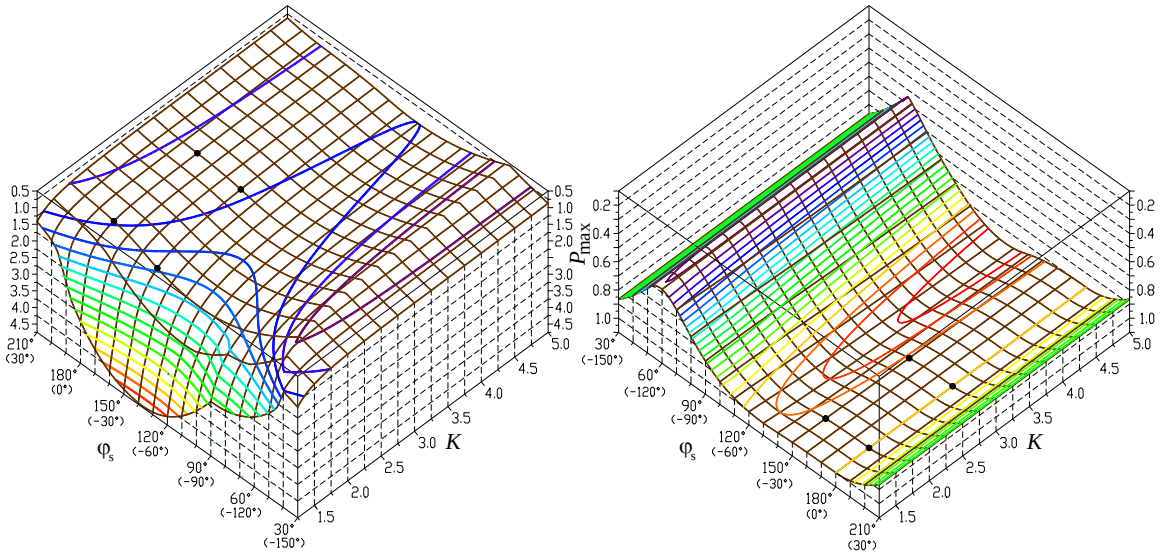

(SR) (LR)

Fig. 8: Peak actuator force of the optimum RPRR mechanisms with Δφ=60°.

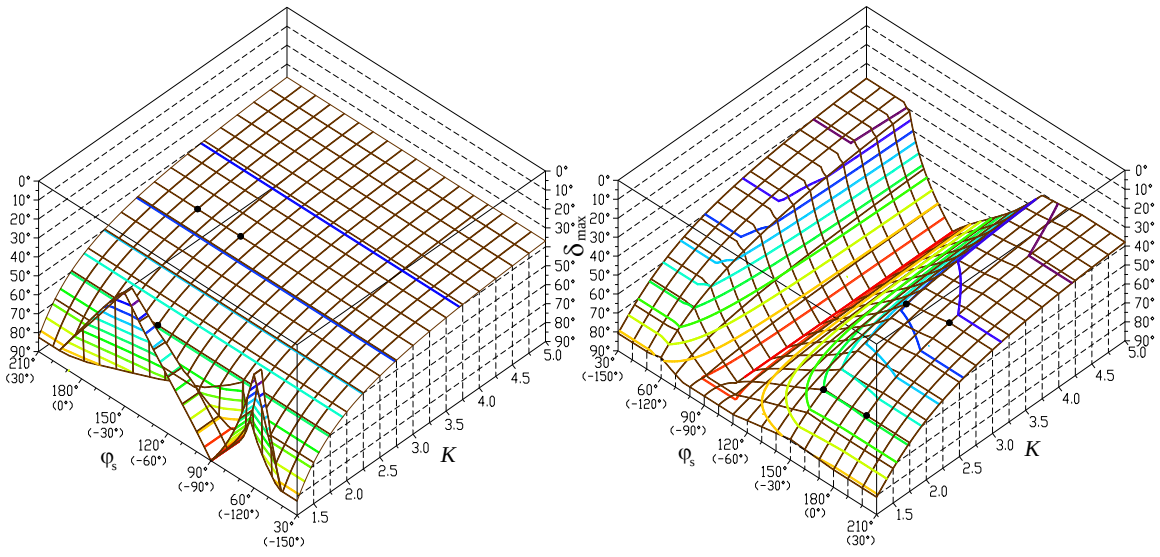

(SR) (LR)

Fig. 9: Maximum deviation from 90° of the transmission angle of optimum RPRR mechanisms with Δφ=60°.

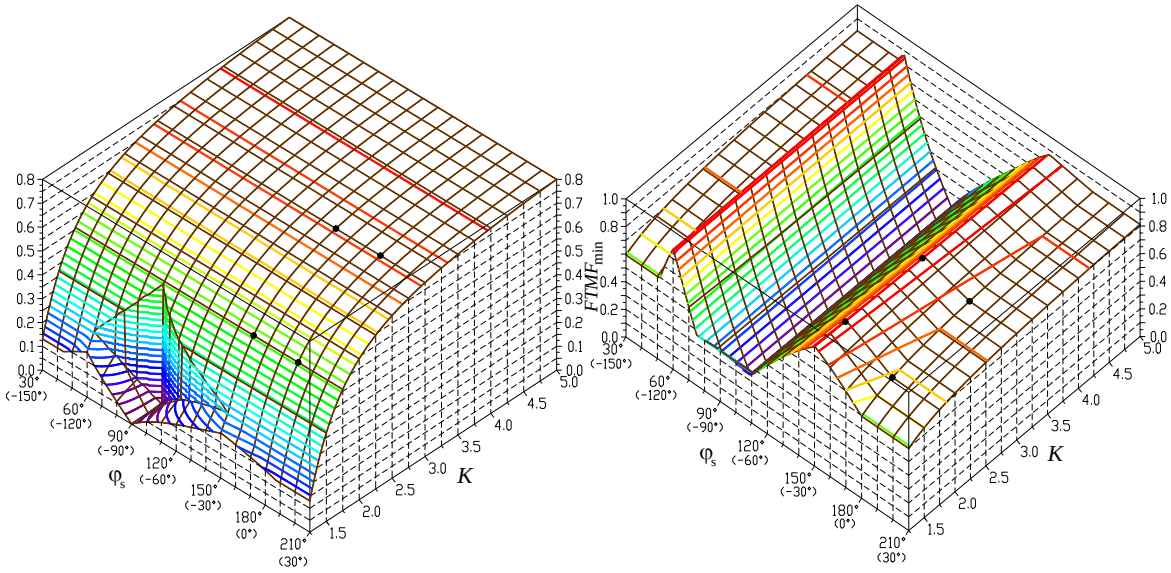

(SR) (LR)

Fig. 10: Maximum *MA* of the optimum RPRR mechanisms with Δφ=60°.

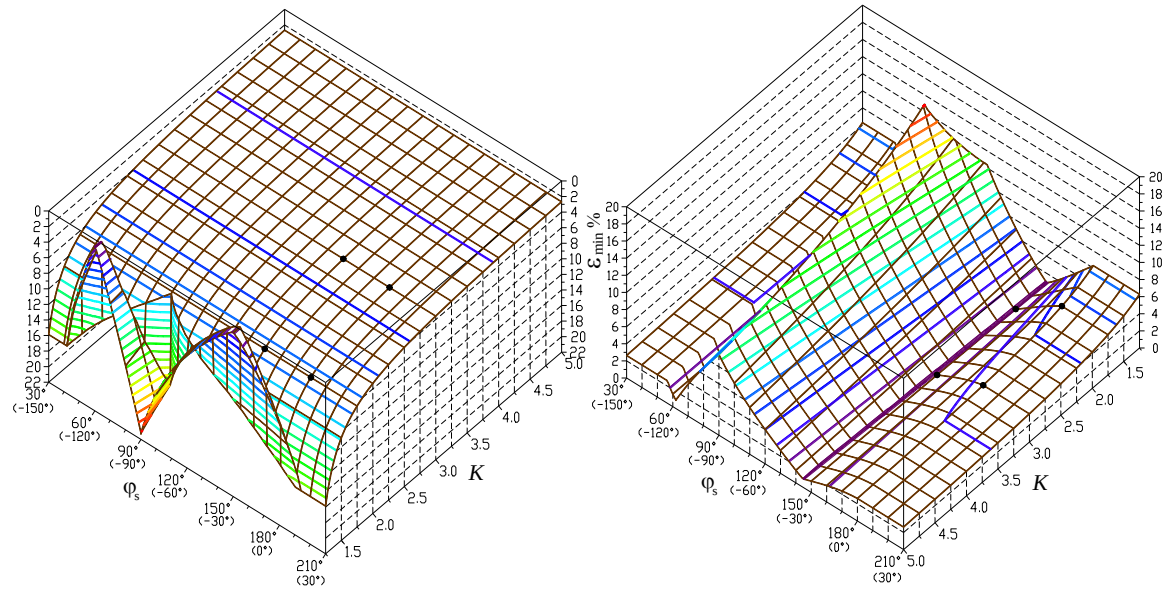

(SR) (LR)

Fig. 11: Maximum I/O linearity error of the optimum RPRR mechanisms with Δφ=60°.

TABLE 2: PARAMETERS OF THE OPTIMUM RPRR MECHANISMS WITH Δφ=60°, φ_s=0°, *K*=1.75 AND *K*=3.

	Type	*K*	*OA*	α	*OB*	AB_s	P_{max}	δ_{max}	ε_{max}	MA_{min}
(a)	SR	1.75	1.0	58.987°	1.0	0.98466	1.2196	59.49°	6.48%	0.508
(b)	SR	3.0	1.0	26.374	1.0	0.45625	1.0367	43.19°	3.55%	0.729
(c)	LR	1.75	1.0	50.957°	1.58755	1.23301	1.0000	64.36°	4.69 %	0.687
(d)	LR	3.0	1.0	25.548°	1.10837	0.47801	1.0000	45.95°	3.29%	0.771

TABLE 3: PARAMETERS OF OPTIMUM RPRR MECHANISMS WITH Δφ=60°, φ_s=–30°, K=1.75 AND K=3.

	Type	*K*	*OA*	α	*OB*	AB_s	P_{max}	δ_{max}	ε_{max}	MA_{min}
(a)	SR	1.75	1.0	88.987°	1.0	0.98466	1.7060	59.49°	6.48%	0.508
(b)	SR	3.0	1.0	56.374°	1.0	0.45625	1.1962	43.19°	3.55%	0.729
(c)	LR	1.75	1.0	64.108°	2.03754	1.33321	1.0105	65.13°	1.01%	0.857
(d)	LR	3.0	1.0	48.549°	1.33367	0.49991	1.0204	50.48°	1.16%	0.849

According to Fig. 5, if an improved transmission angle μ is desired, one should increase *K* and, if possible, reduce the rocker angle Δφ. Same applies if an increased mechanical advantage *MA* or reduced linearity-error ε is desired (see Figs. 6 and 7). The proportions of the corresponding RPRR mechanism with $\varphi_s = 0$ and Δφ between 30° and 120°, optimized for minimum actuator force can be extracted from the parametric charts in Figs. A1, A2 and A3. The accuracy of the parameters thus extracted can be checked by evaluating objective function $Max|P_i(\alpha)|$ supplied as pseudocode in Appendix 1. The same function available as pseudocode in Appendix 1 can be used in the design of optimum actuator force RPRR mechanisms, for the cases

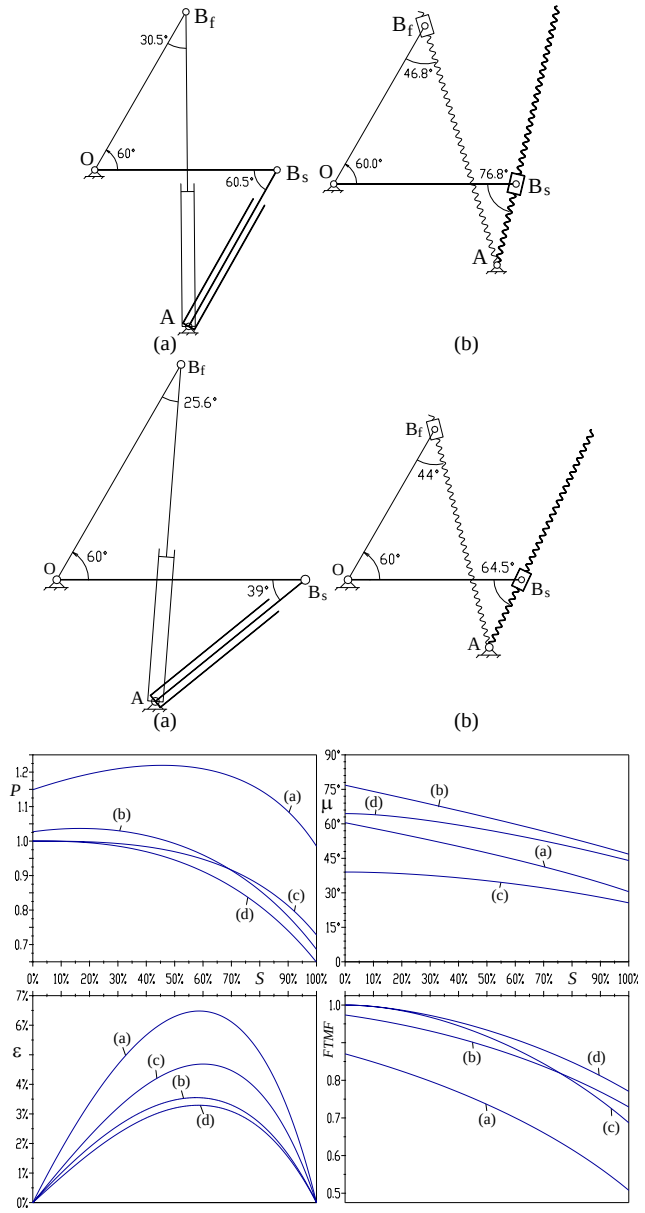

Fig. 12. Kinematic and diagrams (above) and limit positions of the mechanisms in Table 2 and Fig. 12 with the same (a) to (d) labeling.

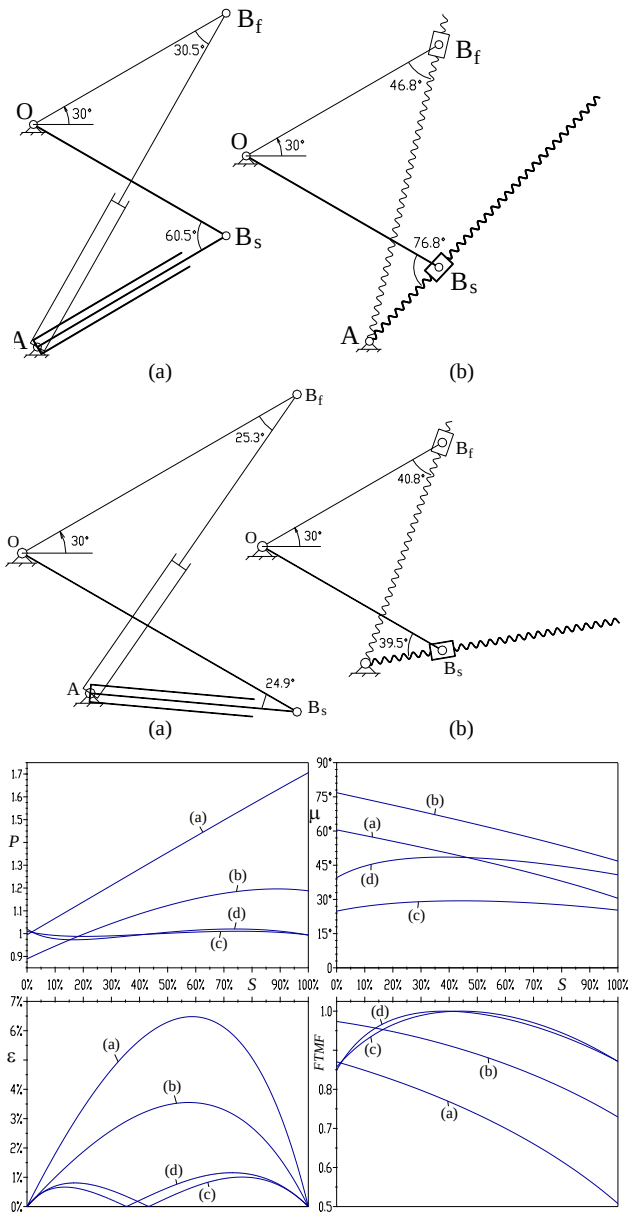

Fig. 13. Kinematic and performance diagrams of the mechanisms in Table 3 and Fig. 14. Labels match the respective figure and table.

where the initial position of the rocker is other than horizontal (i.e. $\varphi_s \neq 0$).

For a better insight into this type of problems, a second set of parametric studies have been performed by minimizing objective function (7) for a fixed angle of swing $\Delta\varphi=60°$, and for $30° \le \varphi_s \le 210°$, and $1.25 \le K \le 5$. The performance plots in Figs. 8, 9, 10 and 11, and the parametric plots in Figs. A4, A5 and A6 are summaries of the results obtained. As stated earlier with reference to Figs. 2-a and b, the design space of the objective function $Max|P_j(\alpha)|$ is periodic with respect to φ_s with a period of 180°. Consequently, the initial rocker angle in Figs. 8 to 11 and A4, A5 and A6 in Appendix 2 can be substituted with $\varphi_s \pm 180°$ (see the φ_s values shown between parentheses on these plots) while angle α should be changed into $\alpha \pm 180°$, which is equivalent to rotating the entire mechanism in Fig. 2 about point O by ±180°.

The following additional design recommendations have been formulated based on the parametric plots in Figs. 8 to 11 and A4 to A6:

1. To reduce the overall actuator force of a SR RPRR mechanism, the designer must increase K, or switch to a LR RPRR mechanism configuration (Fig. 8).

2. Increasing K will improve the transmission angle of both short and LR RPRR mechanisms (Fig. 9).

3. The maximum transmission angle deviation from 90°, maximum mechanical advantage and maximum linearity error of the optimum SR RPRR mechanisms with extension coefficient K greater than 1.75 do not depend on the initial rocker angle φ_s (see Fig. 10 and 11).

The proportions of the RPRR mechanism with $\Delta\varphi=60°$ and φ_s between 30° and 210° (or $-150° \le \varphi_s \le 30°$) with optimum actuator force can be extracted from the parametric charts in Figs. A4, A5 and A6. If a different angle $\Delta\varphi$ is imposed in a design problem, then objective function $Max|P_j(\alpha)|$ available as pseudocode in Appendix 1 can be minimized anew, using for an initial guess values extracted from the chart in Fig. A4.

Fig. 14: Lower position and maximum elevated position of the mast of a drilling research equipment [6].

IV. 4. Numerical Examples

To complement the bivariate plots in Figs. 4 to 11 and in Appendices 1 and 2, several numerical examples of RPRR mechanisms optimized for actuator force are discussed next. These are RPRR mechanisms of the SR and LR type with $\Delta\varphi$=60°, driven by linear actuators with K=1.75 and K=3, and with initial rocker angles φ_s=0 and φ_s=150° (as explained earlier, φ_s=150° is equivalent to φ_s=-30°). Their optimum geometric parameters are summarized in Tables 2 and 3.

The mechanisms with the parameters in Tables 2 and 3 are shown in their limit positions in Figs. 12 and 13. Animated GIFs of these mechanisms, where their LR versions appear driven by power screws, are available for download from [36]. Figs. 12 and 13 also show the I/O function φ(S), transmission angle μ(S), displacement linearity error ε(S) and force-to-torque multiplication factor *MA*(S) companions to Figs. 12 and 14. For conformity, their parameters have been marked with dots on the bivariate plots in Figs. 4 to 11 and in Appendices 1 and 2.

V. Conclusion

An optimization problem has been formulated and solved numerically for the RPRR mechanism loaded by downward gravitational forces only, having as objective minimizing the maximum actuator force. Bivariate parametric design charts and transmission angle, mechanical advantage and input-output linearity error performance charts have been generated by repeating this optimization problem. These charts allow for an overview upon the capabilities of the RPRR mechanism, useful in the design situations when the angle of swing of the rocker $\Delta\varphi$, or/and the extension coefficient K of the linear actuator do not have strictly imposed values. Also provided in Appendix 1 to the paper is the pseudocode of the objective function which served to generate the above-mentioned charts, useful to the practicing engineer in refining the solution to his/her own problem.

The results reported and the design results summarized in the charts presented herein are believed to be of significant practical value. Without a doubt, lifting-equipment companies have developed techniques for the optimum design of their products, but these are seldomly published. O the other hand, an optimization subroutine alone provides little overview upon the design alternatives available, in comparison with the numerous parametric charts in this paper. It is believed that the publication of these charts could spare future design errors, like the multi-million dollar facility pictured in Fig. 14, which includes a mast that was supposed to elevate close to 90°, but due to the improper actuator positioning, it does not elevate more than 40°.

Appendix 1

Pseudocode of the objective function in equation (7) and of auxiliary functions Max3 and S123.

```
FUNCTION Max3(r1,r2,r3)  //Returns the maximum of r1,r2 and r3
 IF r1 > r2 THEN Max3 ← r1 ELSE Max3 ← r2 END ELSE
 IF Max3 < r3 THEN Max3 ← r3 END ELSE
RETURN
FUNCTION S123(x1,y1,x2,y2,x3,y3)
//If loop 1–2–3 is oriented CCW then S123 > 0 else S123 < 0
 S123 ← (x2–x1)*(y3–y1)–(y2–y1)*(x3–x1)
RETURN
FUNCTION maxPj(ALPHA, PHIs, DPHI, K, PlsMns)
//Returns the maximum absolute value of the actuator force Pj.
//Angles ALPHA, PHIs and DPHI must be in radians.
//For long rocker PlsMns=1 while for short rocker and PlsMns=–1
 MaxPj ← 1E100  //large function value returned by default
 cPHIs ← cos(PHIs+ALPHA)
 sPHIs ← sin(PHIs+ALPHA)
 cPHIf ← cos(PHIs+ALPHA+DPHI)
 sPHIf ← sin(PHIs+ALPHA+DPHI)
 RR ← (K^2*cPHIs–cPHIf)/(Sqr(K)–1)
 IF RR^2–1 < 0 THEN RETURN
 OB ← RR+PlsMns*Sqrt(RR^2–1)
 IF OB ≤ 0 THEN RETURN
 OBAs ← S123(0,0,cPHIs*OB,sPHIs*OB,1,0)
 OBAf ← S123(0,0,cPHIf*OB,sPHIf*OB,1,0)
 IF OBAs*OBAf < 0 THEN RETURN  //Avoids branch defects
 ABs ← OB^2–2*OB*cPHIs+1
 IF ABs ≤ 0 THEN RETURN
 ABs ← Sqrt(ABs)
 ABf ← K*ABs
 IF 2*Max3(OB,ABs,1) > OB+ABs+1 THEN RETURN
 IF 2*Max3(OB,ABf,1) > OB+ABf+1 THEN RETURN
 MaxPj ← –1E100
 n ← Round(5*DPHI*180/Pi)  //number of intermediate displacements
 FOR j ← 0 to n DO
  ABj ← ABs+(ABf–ABs)*j/n
  cPHIj ← (OB^2–ABj^2+1)/(2*OB)
  PHIj ← ArcTan(Sqrt(1–cPHIj^2)/cPHIj)
  cPHIj ← cos(PHIj–ALPHA)
  cMUj ← (OB^2+ABj^2–1)/(2*OB*ABj)
  if Abs(cMUj) ≥ 1 then RETURN
  Pj ← Abs(cPHIj/(OB*Sqrt(1–cMUj^2)))
  if (Pj > MaxPj) then MaxPj ← Pj
 END FOR
RETURN
```

APPENDIX 2:

Geometric parameters of the normalized RPRR oscillating-slide mechanisms with $\varphi_s=0$, $30° \le \Delta\varphi_s \le 120°$ and $1.25 \le K \le 5$ optimized for *mini-max* actuator force.

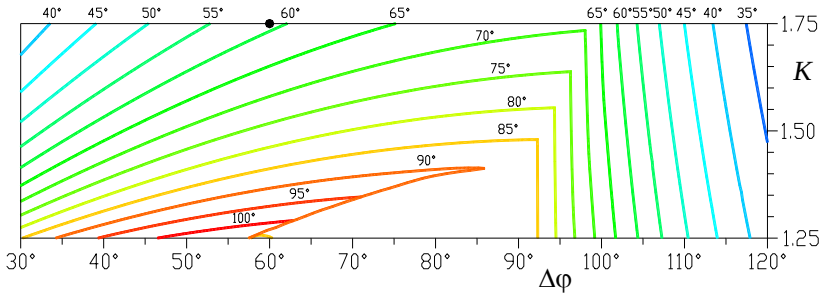

(SR)

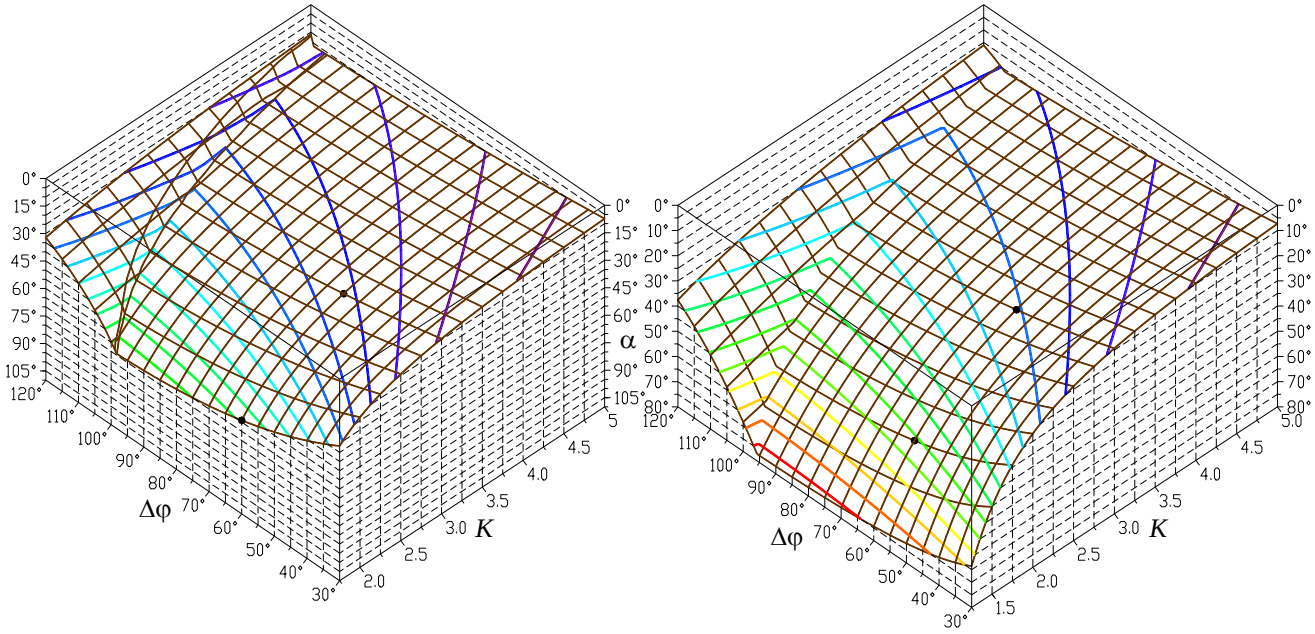

Fig. A1: Optimum angle α of the RPRR mechanisms with $\varphi_s=0$.

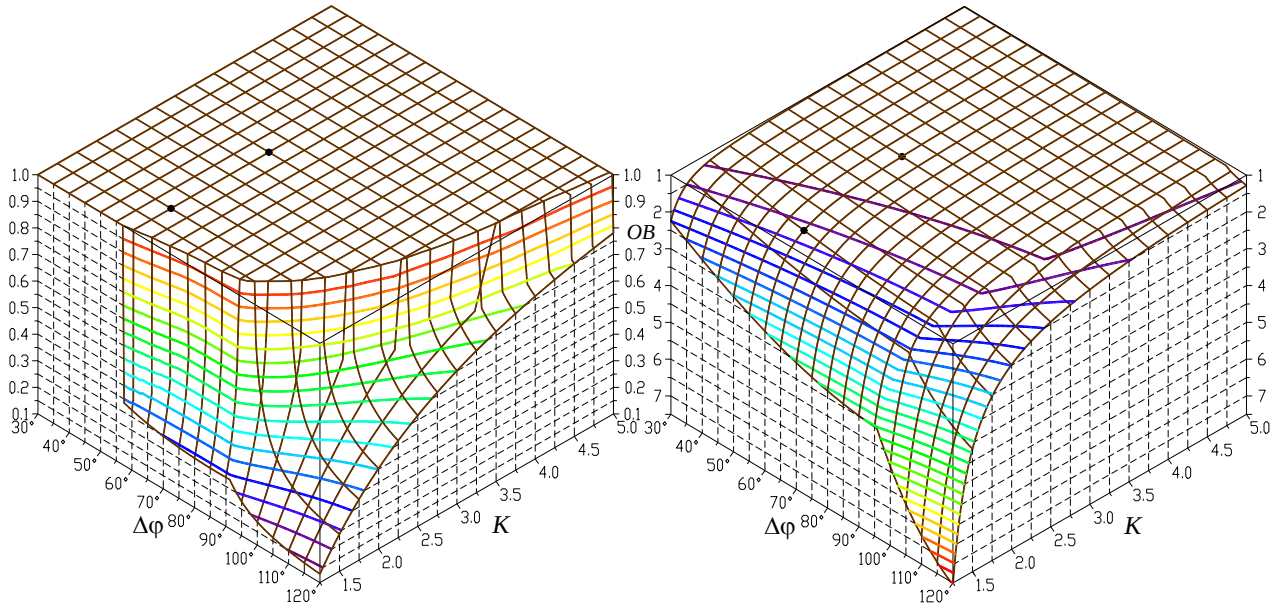

Fig. A2: Optimum normalized rocker length of the RPRR mechanisms with $\varphi_s=0$.

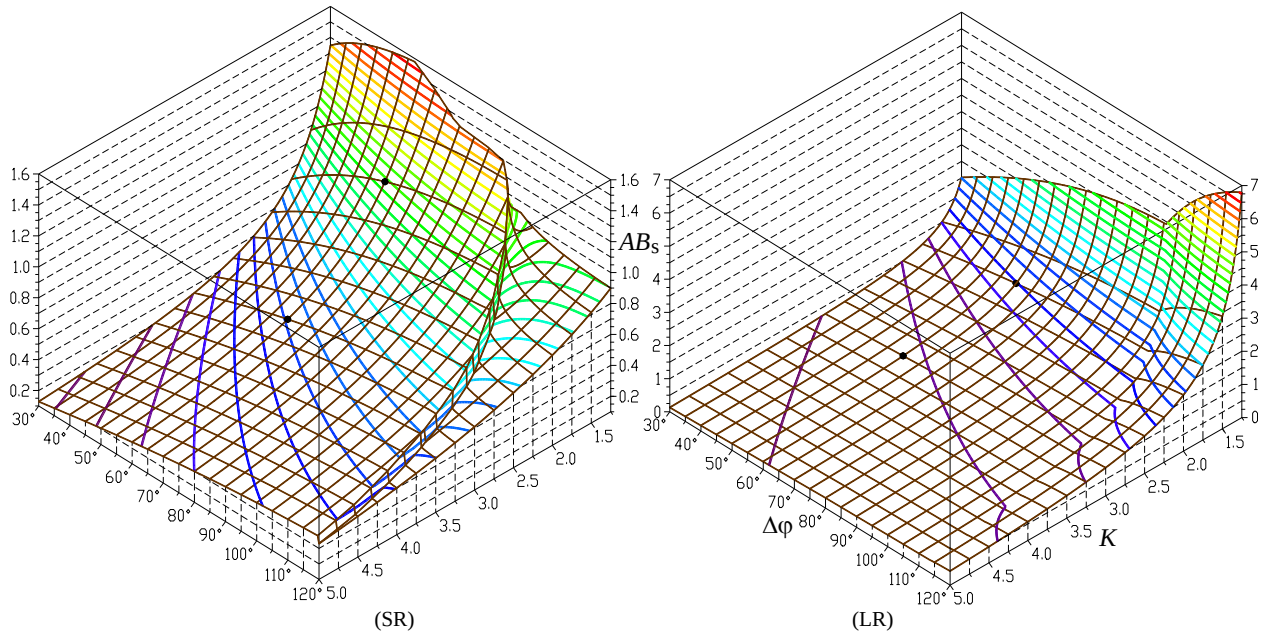

Fig. A3: Optimum initial actuator length (normalized) of the RPRR mechanisms with φ_s=0. Plot (**a**) corresponds to short rocker mechanisms and plot (**b**) corresponds to long rocker mechanisms.

APPENDIX 3:

Geometric parameters of the normalized RPRR oscillating-slide mechanisms with $\Delta\varphi$=60°, 30° ≤ φ_s ≤ 210° (or -150° ≤ φ_s ≤ 30°) and 1.25 ≤ K ≤ 5 optimized for mini-max actuator force.

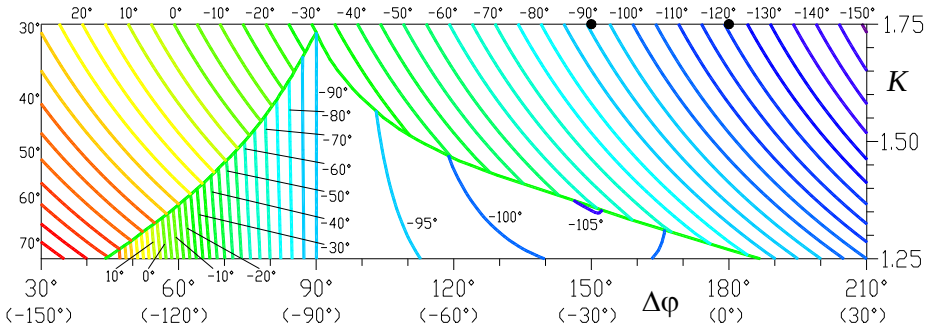

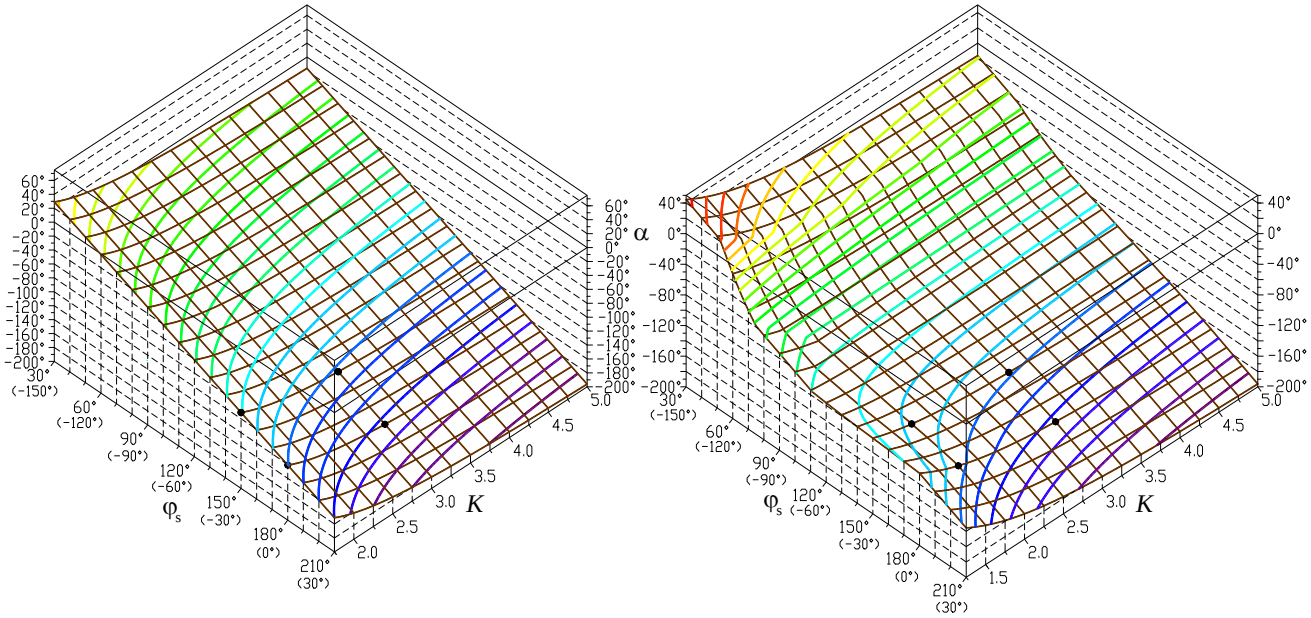

Fig. A4: Optimum angle α of the RPRR mechanisms with $\Delta\varphi_s$=60°. If the φ_s values in parentheses are used, then angle α extracted from the chart should be change to α-180°.

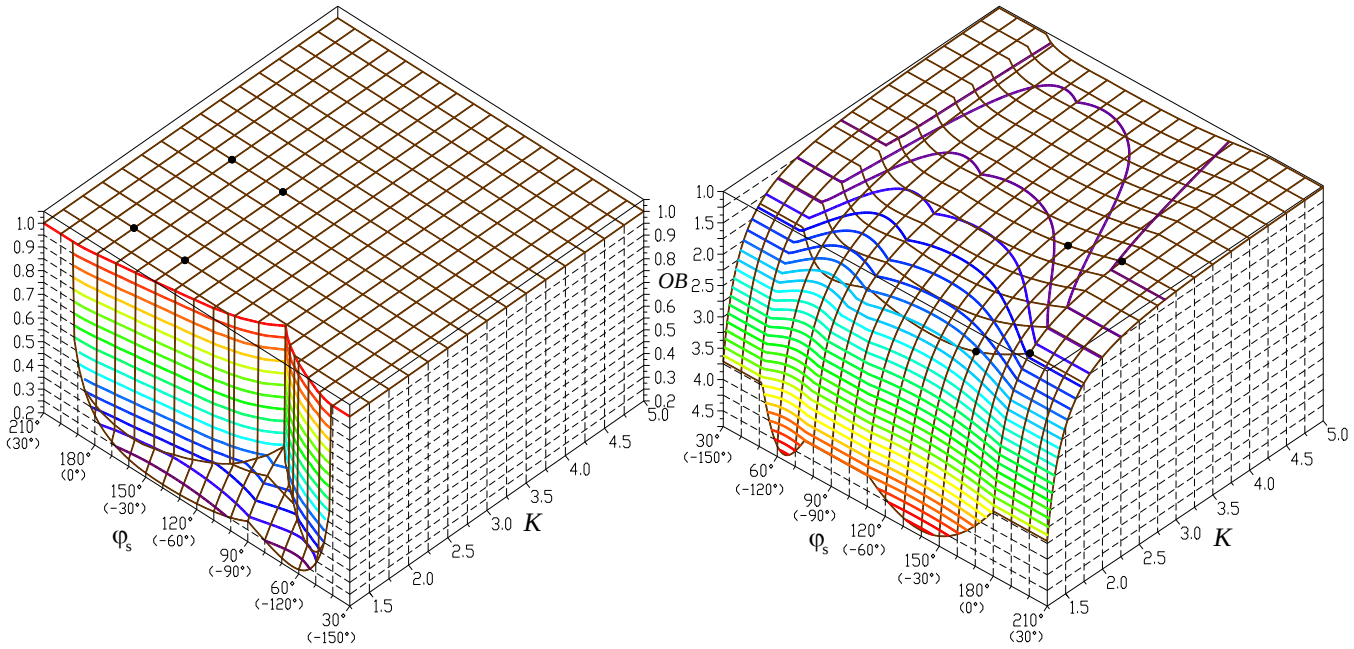

Fig. A5: Optimum normalized rocker length of the RPRR mechanisms with $\Delta\varphi_s$=60°.

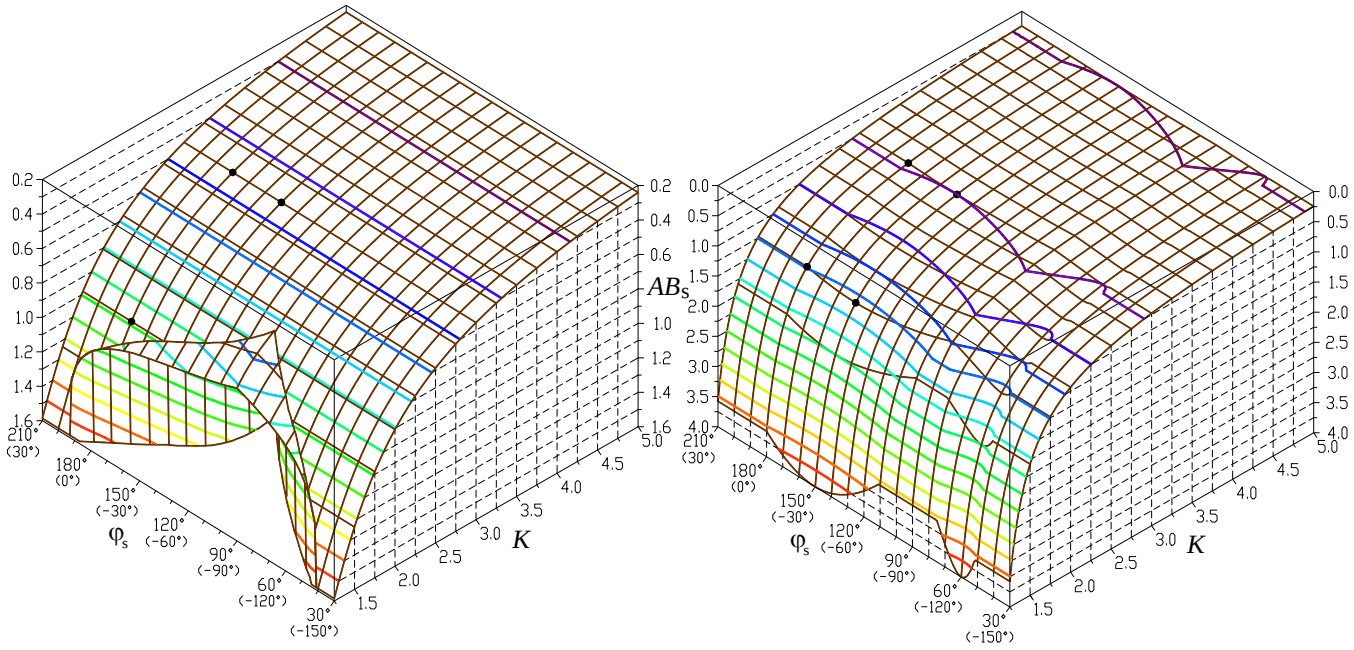

Fig. A6: Optimum initial actuator length (normalized) the RPRR mechanisms with $\Delta\varphi_s$=60°.

REFERENCES

[1] Hain K. 1960 "Die Bedeutung eines Getriebeatlasses über Vierwinkelfunctionen von Gelenkvierecken an Hand von Beispielen aus dem Landmaschinenbau", Grundlagen der Landtechnik, Heft 12, p. 37-45

[2] Hain K. 1968 "Zur Weiterentwicklung der Ladegeräte mit hydraulischen Schubkolbenantrieben", Landbauforschung Völkenrode, 18, p. 79-82

[3] Söylemez E. 2009 Mechanisms, Middle East Technical University, METU Publication #64, Ankara, Turkey.

[4] Norton R.L. 2011 Design of Machinery, McGraw-Hill Education, New York, USA.

[5] Bye R.T., Osen O.L. and Pedersen B.S. 2015 "A Computer-Automated Design Tool for Intelligent Virtual Prototyping of Offshore Cranes", Proc. of the 29th European Conference on Modelling and Simulation, ECMS 2015, Albena (Varna), Bulgaria.

[6] Chennamsetty V.K. and Simionescu P.A 2006 "Modification of the ACTF Loop Elevation System", The University of Tulsa Drilling Research Projects Advisory Board Meeting, May 2006, Tulsa, OK, USA, p. 12.

[7] Invacare Corp. 2019 Catalog, Elyria, OH, USA

[8] Konecranes Plc. 2019 Catalog, Hyvinkää, Finland.

[9] Parker Hannifin Corp. 2009 Catalog HY18-0014, Youngstown, OH, USA.

[10] Hartenberg R.S. and Denavit J. 1964 Kinematic Synthesis of Linkages, McGraw-Hill, New York, USA

[11] Tao D.C. 1964 Applied Linkage Synthesis, Addison-Wesley, Boston, MA, USA

[12] Volmer J. 1978 Getriebetechnik Leitfaden, Vieweg & Teubner Verlag, Braunschweig, Germany.

[13] Bagci C. 1987 "Synthesis of Linkages to Generate Specified Histories of Forces and Torques - The Planar 4R Four-Bar Mechanism", Proc. of the ASME Design Technology Conference, Boston, MA, Sept. 27-30, 1987, 10-2, p. 227 236.

[14] Bagci C. 1987 "Synthesis of Linkages to Generate Specified Histories of Forces and Torques - The Planar Slider-Rocker Mechanism", Proc.

of the ASME Design Technology Conference, Boston, MA, Sept. 27-30, 1987, 10-2, p. 237 244.

[15] Lin C.C. and Chang W.T. 2002 "The Force Transmissivity Index of Planar Linkage Mechanisms", Mechanism and Machine Theory, 37(12), p. 1465–1485

[16] Yu W.-J., Huang C.-F. and Chieng W.-H. 2004 "Design of the Swinging-Block and Turning-Block Mechanism with Special Reference to the Mechanical Advantage", JSME International Journal, Series C, 47(1), p. 363-368.

[17] Gerasimov Yu. Yu. and Siounev V.S. 2000, "Forest Machinery Crane Compound Scheme Synthesis: Optimization of Hydraulic Cylinder Operating Mechanisms", International Journal of Forest Engineering, 11(1), p. 73-79.

[18] Harl B., Oblak M. and Butinar B., 2004, "Minimization of joint reaction forces of kinematic chains by a multi-objective approach", Structural and Multidisciplinary Optimization, 27(4), p 243–249.

[19] Sandor G.N. and Erdman A.G. 1984 Advanced Mechanism Design: Analysis and Synthesis, Prentice Hall, Upper Saddle River, NJ, USA

[20] Simionescu P.A. and Smith M.R. (2000) "Single-valued Function Representations in Linkage Mechanisms Design", Mechanism and Machine Theory, 35(12), p. 1709–1726.

[21] Shoup T.E. 1978 Practical Guide to Computer Methods for Engineers, Prentice Hall, Englewood Cliffs, NJ, USA

[22] Beiner L. 1995 "A minimax problem of optimal actuator placement for lifting", Proc. of the IUTAM Symposium on Optimization of Mechanical Systems, Stuttgart, Germany, 26-31 March.

[23] Huang, C., and Roth, B., 1993, "Dimensional Synthesis of Closed-loop Linkages to Match Force and Position Specifications," ASME Journal of Mechanical Design, 115(2) p. 194–198.

[24] Scardina, M. T., Soper, R. R., Calkins, J. M., and Reinholtz, C., 1995, "Optimal Synthesis of Force Generating Planar Four-link Mechanisms," Proceedings of the 4th National Applied Mechanisms and Robotics Conference, Cincinnati, OH, Paper No. AMR 95-003.

[25] Krovi V., Ananthasuresh G.K. and Kumar V. 2002, "Kinematic and Kinetostatic Synthesis of Planar Coupled Serial Chain Mechanisms," ASME Journal of Mechanical Design, 124(2), p. 301-312.

[26] Simionescu P.A. 2016 "Design of planar slider-rocker mechanisms for imposed limit positions, with transmission angle and uniform motion controls", Mechanism and Machine Theory, 97, p. 85–99.

[27] Texas Hydraulics Inc. 2019 Catalog, Temple, TX, USA

[28] Ergo-Help Pneumatic Inc. 2019 Catalog, Arlington Heights, IL, USA

[29] Eagle Hydraulic Components Inc. 2019 Catalog, Mirabel, QC, Canada

[30] Heinze A. 2007 Modelling, simulation and control of a hydraulic crane, MS Thesis, Växjö University, Sweden, 135 p.

[31] Reifschneider L.G. 2005 "Teaching Kinematic Synthesis of Linkages without Complex Mathematics", Journal of Industrial Technology, 21(4), p. 1-16.

[32] Binh, N.T. 2016 "Smoothed lower order penalty function for constrained optimization problems" IAENG International Journal of Applied Mathematics, 46(1), p. 76–81.

[33] Beiner L. 1997 "Minimum force redundancy control of hydraulic cranes" Mechatronics, 7(6), p. 537-547.

[34] Brent R.P. 2013 Algorithms for Minimization without Derivatives, Dover Publications, Mineola, NY, USA

[35] Simionescu P.A. 2014 Computer-Aided Graphing and Simulation Tools for AutoCAD Users, Chapman & Hall/CRC, Boca Raton, FL, USA

[36] ResearchGate Supplementary Resource, 2020, Animated GIFs for "Parametric Studies for the Optimum Synthesis of Oscillating-Slide Actuators for Vertical Manipulation Applications", DOI: 10.13140/RG.2.2.29910.75841

Petru A. Simionescu (M'18) This author became a member of IAENG in 2018. He received a BS degree in mechanical engineering from University Politehnica of Bucharest in 1992, and a doctorate in technical sciences, from the same university in 1999. In 2004 he received a PhD degree in mechanical engineering with an applied mathematics minor from Auburn University, USA. Currently he is on the engineering faculty at Texas A&M University in Corpus Christi. He is also a registered Professional Engineer in the Sate of Texas. Simionescu taught and conducted research at seven Romanian, British, and American universities, and worked for four years in industry as an automotive engineer. His research interests include kinematics, dynamics and design of multibody systems, evolutionary computation, CAD, computer graphics, and information visualization. So far, has authored one book (see reference [35] above), more than 60 technical papers and has been granted nine patents.

MODIFICATIONS:

Corrected three typos in the Abstract (shown in red below) DATE 07/27/2020

Updated Reference [36] to reflect the current title of the paper. DATE 07/27/2020

***Abstract*—The oscillating-slide linkage, symbolized RPRR is one of the most utilized inversions of the slider-crank mechanism. This paper considers the cases where the rocker of an RPRR mechanism is loaded primarily by gravitational forces, like in boom cranes, dump trucks and aerial-work platforms. In all these applications, in addition to satisfying imposed limit positions, minimizing the peak actuator force over the working range of the mechanism is the main requirement. An optimization problem is defined and the dual solutions to this problem i.e. a short-rocker and a long-rocker RPRR mechanism, are summarized in the form of parametric charts, ~~and~~ performance charts and design recommendations. Also observed via bivariate plots are the ensuing transmission angle, mechanical advantage and input-output linearity error of these optimum mechanism solutions. Together, these plots (each consisting of thousands of points obtained through repeated optimization) allow for a rapid overview upon the capabilities of the RPRR mechanism, being additionally useful in guiding the designer's decision when flexibility exists in choosing the extension coefficient of the actuator, or the angle of swing of the rocker is not imposed a strict value.**